Engineering of Saccharomyces cerevisiae for enhanced metabolic robustness and L-lactic acid production from lignocellulosic biomass

(article starts on next page)

Engineering of *Saccharomyces cerevisiae* for enhanced metabolic robustness and L-lactic acid production from lignocellulosic biomass

Bohyun Choi [a], Albert Tafur Rangel [b,c], Eduard J. Kerkhoven [b,c,d], Yvonne Nygård [a,e,*]

[a] *Department of Life Sciences, Industrial Biotechnology, Chalmers University of Technology, Gothenburg, Sweden*
[b] *Department of Life Sciences, Systems and Synthetic Biology, Chalmers University of Technology, Gothenburg, Sweden*
[c] *Novo Nordisk Foundation Center for Biosustainability, Technical University of Denmark, Kgs. Lyngby, Denmark*
[d] *SciLifeLab, Chalmers University of Technology, Gothenburg, Sweden*
[e] *VTT Technical Research Centre of Finland Ltd, Espoo, Finland*

A B S T R A C T

Metabolic engineering for high productivity and increased robustness is needed to enable sustainable bio-manufacturing of lactic acid from lignocellulosic biomass. Lactic acid is an important commodity chemical used for instance as a monomer for production of polylactic acid, a biodegradable polymer. Here, rational and model-based optimization was used to engineer a diploid, xylose fermenting *Saccharomyces cerevisiae* strain to produce L-lactic acid. The metabolic flux was steered towards lactic acid through the introduction of multiple lactate dehydrogenase encoding genes while deleting *ERF2*, *GPD1*, and *CYB2*. A production of 93 g/L of lactic acid with a yield of 0.84 g/g was achieved using xylose as the carbon source. To increase xylose utilization and reduce acetic acid synthesis, *PHO13* and *ALD6* were also deleted from the strain. Finally, *CDC19* encoding a pyruvate kinase was overexpressed, resulting in a yield of 0.75 g lactic acid/g sugars consumed, when the substrate used was a synthetic lignocellulosic hydrolysate medium, containing hexoses, pentoses and inhibitors such as acetate and furfural. Notably, modeling also provided leads for understanding the influence of oxygen in lactic acid production. High lactic acid production from xylose, at oxygen-limitation could be explained by a reduced flux through the oxidative phosphorylation pathway. On the contrast, higher oxygen levels were beneficial for lactic acid production with the synthetic hydrolysate medium, likely as higher ATP concentrations are needed for tolerating the inhibitors therein. The work highlights the potential of *S. cerevisiae* for industrial production of lactic acid from lignocellulosic biomass.

1. Introduction

Lactic acid is an organic acid with a wide range of applications in the food, chemical, pharmaceutical and cosmetics industries. Moreover, lactic acid can be polymerized into polylactic acid (PLA), a raw material for biodegradable plastics. Lactic acid is today produced commercially both through chemical synthesis and biological fermentation. Biological production can provide optically pure D- or L-lactic acid depending on the lactate dehydrogenase (LDH) of the production organism, whereas chemical synthesis generates a racemic mixture of D/L-lactic acid (Yankov, 2022). Current commercial production of lactic acid relies on sugars derived from sugarcane or corn starch (Singh et al., 2022). Still, the utilization of sugars derived from lignocellulosic biomass as a substrate for lactic acid has been demonstrated with various

microorganisms, counting lactic acid bacteria and native lactic acid producing fungi such as *Rhizopus oryzae* and *Rhizopus arrhizus* (Ojo and de Smidt, 2023; Yankov, 2022). Many organisms have been genetically modified to produce lactic acid, including yeasts such as *Saccharomyces cerevisiae*, several *Candida* sp. and some *Kluyveromyces* sp. (Ojo and de Smidt, 2023). Extensive research has been conducted to enable *S. cerevisiae* to ferment lignocellulosic hydrolysates. The utilization of both pentoses (xylose and arabinose) and hexoses (glucose, mannose, and galactose) as substrates for lactic acid production is attractive as lignocellulosic biomass is an abundant and underutilized resource (Srivastava et al., 2023). Lactic acid production from lignocellulosic hydrolysates using *S. cerevisiae* as the production host was recently demonstrated (Lam et al., 2021). *S. cerevisiae* that intrinsically shows great robustness, including great pH and acid tolerance, is widely used

---

for the production of various fuels and chemicals. *S. cerevisiae* is an attractive host for lactic acid production as it can overcome major obstacles with using lactic acid bacteria as production hosts, namely issues with phage contamination, requirement for complex nutrients and need for a relatively high pH (Hetényi et al., 2011). Lactic acid fermentation at low pH is preferred to avoid extensive addition of neutralizing agents and subsequent gypsum formation.

Lactic acid production by *S. cerevisiae* requires introduction of an LDH encoding gene. LDHs catalyze the one-step conversion of pyruvate to lactic acid. LDHs of various origin, including *Bos taurus, Lactobacillus plantarum, Lactobacillus casei, Leuconostoc mesenteroides,* or *Rhizopus oryzae* have been shown functional in *S. cerevisiae* (Dequin et al., 1999; Ishida et al., 2006a, 2006c; Skory, 2003; Valli et al., 2006). Expression of multiple copies of LDH encoding genes has led higher lactic acid titers (demonstrated e.g. by Baek et al. (2016), Ishida et al. (2006a) and Turner et al. (2015)). Still, bioproduction by *S. cerevisiae* is typically challenged by ethanol accumulation (Skory, 2003; van Dijken et al., 1993). The challenge of this so-called overflow metabolism, e.g., ethanol production from pyruvate even in the presence of oxygen, has been overcome through deletion of pyruvate decarboxylase (PDC) and/or alcohol dehydrogenase (ADH) encoding genes, but these modifications also cause severe growth defects (Ishida et al., 2006b; Tokuhiro et al., 2009). Evolutionary engineering (van Maris et al., 2004) as well as targeted deletion of a regulatory element of *MTH1,* encoding a transcriptional regulator involved in glucose sensing (Oud et al., 2012) were demonstrated as successful strategies to improve the growth of PDC defect strains on glucose. Even so, growth defects and/or redox imbalance challenge the use of such stains.

To increase the biochemical productivity of *S. cerevisiae*, genome-scale constraint-based metabolic models have been widely used in the prediction of metabolic engineering targets (Han et al., 2023). While classical constraint-based approaches such as OptKnock (Burgard et al., 2003) and Flux Scanning based on Enforced Objective Flux (FSEOF) (Choi et al., 2010) are able to predict gene targets, these approaches do not consider limiting factors such as protein availability and typically generate large numbers of potential genetic interventions. To address this, enzyme-constrained models (ecModels, Kerkhoven (2022)) and the GECKO toolbox, which integrate protein turnover numbers and are able to predict optimal protein allocations (Chen et al., 2024), were developed. This approach drastically reduces the *in-silico* solution space, yielding less predicted targets with higher confidence. Modeling the use of different carbon sources for biochemical production has thus far received less attention.

Xylose assimilation by *S. cerevisiae* has been achieved by heterologous expression of xylose isomerase (XI) or xylose reductase (XR) and xylitol dehydrogenase (XDH) encoding genes. The resulting 5-xylulose can then be further converted via the pentose phosphate pathway to glyceraldehyde-3-phosphate that is through glycolysis converted into pyruvate. Despite numerous efforts including both evolutionary engineering and targeted strain improvement, xylose fermentation by engineered *S. cerevisiae* remains a challenge. In medium with mixed carbon sources xylose is typically utilized only after glucose is depleted, which can be attributed both to challenges in xylose uptake and efficiency of the xylose metabolic pathways. The XR-XDH pathway (encoded by *XYL1* and *XYL2*) that is used by many xylose-fermenting yeasts has a thermodynamic advantage compared to the XI pathway (Karhumaa et al., 2007) whereas the cofactor imbalance between the mainly NADPH-dependent XR and the NAD$^+$-dependent XDH often provokes xylitol accumulation (Lee et al., 2021). Efforts to increase xylose consumption include fine turning the expression of *XYL1, XYL2,* and *XYL3* (xylose kinase from *S. stipites*) (Kim et al., 2013), deletion of *GRE3* encoding an aldose reductase (Sato et al., 2016), deletion of *PHO13* encoding a phosphatase (Bamba et al., 2016) or deletion of *ALD6* encoding an acetaldehyde dehydrogenase (Kim et al., 2013). Moreover, redox cofactor regeneration (Verho et al., 2003), xylose uptake (Jin et al., 2005), or expression of heterologous xylose transporters (Reider

Apel et al., 2016) has been attempted. The CEN.PK XXX strain utilized in this study was engineered to overexpress the native *RPE1*, *TAL1*, *RKI1*, *TKL1* and *XKS1* genes, and codon optimized *XYL1* and *XYL2* from *Scheffersomyces stipites* (Westman et al., 2014). In our recent work, we used a CEN.PK XXX derived strain to produce lactic acid when co-cultured with *Acinetobacter baylyi* ADP1, a bacterium capable of detoxifying inhibitors of lignocellulosic hydrolysates (Liu et al., 2024).

In this study, we combined rational engineering with enzyme constrained metabolic modeling. The constructed *S. cerevisiae* strain expressed six LDH encoding genes from *B. taurus* and was engineered on the one hand for improved redox-balance and on the other hand for increased xylose assimilation and strain robustness. The resulting, highly acid tolerant and highly lactic acid producing strain provides a robust cell factory for lactic acid production from lignocellulosic feedstocks.

2. Materials and methods

2.1. Media and culture conditions

S. cerevisiae was cultured in medium containing 10 g/L yeast extract, 20 g/L peptone, and carbon sources as indicated when describing the different experiments, YPD for 20 and 50 g/L D-glucose and YPX for 20, 40, 50, 60, 90, 120, and 130 g/L D-xylose, sometimes solidified with 20 g/L agar. The initial pH of the YPD and YPX media was 6.8. Geneticin (Fisher Scientific, MA, USA) was added to the solidified agar medium at a concentration of 200 μg/L for screening of recombinant strains harboring plasmids expressing *Cas9* (pYN2_1 (Addgene #184757, Camara et al. (2020)) and BC01-BC05). The synthetic lignocellulosic hydrolysate (SLH) medium composition was set to mimic spruce hydrolysate (Nickel, 2021). The SLH medium contained 12.2 g/L glucose, 7.9 g/L xylose, 10.4 g/L mannose, 7.1 g/L galactose, 2.8 g/L arabinose, 2.7 g/L acetic acid, 0.3 g/L formic acid, 5 g/L yeast extract, 2.5 g/L urea, 2.5 g/L (NH$_4$)$_2$SO$_4$, 0.9 g/L furfural, 0.4 g/L hydroxymethylfurfural (HMF), 0.5 g/L ferulate, and 0.5 g/L *p*-coumarate. Modified SLH medium lacking furfural, HMF, ferulate and p-coumarate was used for bioreactor fermentations and precultures for these. The pH of the SLH medium was adjusted to 6.0 using 2 M NaOH. Calcium carbonate (CaCO$_3$) was used as a neutralizing agent in flask fermentation and added at 10 g/L when supplied sugar concentration was less than 40 g/L, at 20 g/L when the sugar concentration was 40–90 g/L, and at 30 g/L when the sugar concentration exceeded 90 g/L. As high concentrations of calcium lactate (>100 g/L) have been shown to be inhibitory for microbes (Hetényi et al., 2011), we limited the amount of CaCO$_3$ to match the lactic acid production. The amount of CaCO$_3$ added was determined through preliminary experiments, where the presence or absence of CaCO$_3$ remaining at the point of maximum lactic acid production was monitored. *S. cerevisiae* stock cultures were stored in 1:1 ratio of 50 % glycerol solution and YPX medium (20 g/L xylose) and maintained on solid YPX medium (20 g/L xylose).

2.2. Strain construction

The xylose-fermenting *S. cerevisiae* CEN.PK XXX strain (Westman et al., 2014) was used as the parental strain. All yeast strains constructed and used in this study are described in Table 1. The *LDH* gene from *B. taurus* (synthesized by IDT, USA) with codon optimization for *S. cerevisiae* contained flanking restriction enzyme sequences of *Xba*I and *Xma*I. *CDC19* was PCR-amplified from gDNA of *S. cerevisiae* CEN.PK XXX with primers harboring restriction enzyme sequences of *Sal*I and *Bam*HI. *LDH* and *CDC19* expression modules were constructed through restriction-ligation (enzymes from NEB, USA) to the YIplac128--*TEF2p-CYC1t* and YIplac204-*TDH3p-CYC1t* plasmids which are modified from YIplac128 and YIplac204 (Gietz and Sugino, 1988). This way, *LDH* and *CDC19* were put under the control of the *TDH3* and *TEF2* promoters and the *CYC1* terminator, resulting in plasmids YIP_BC01 (Addgene

Table 1
Strains used in this study.

Strain	Description	Source
CEN.PK XXX	*Saccharomyces cerevisiae* CEN.PK 122 MDS, a xylose fermenting strain	Westman et al. (2014)
LX1	CEN.PK XXX *cyb2Δ::P$_{TDH3}$-LDH-T$_{CYC1}$*	This study
LX2	LX1 *erf2Δ::P$_{TEF2}$-LDH-T$_{CYC1}$*	This study
LX3	LX2 *gpd1Δ::P$_{TDH3}$-LDH-T$_{CYC1}$*	This study
LX4	LX3 *Δpho13*	This study
LX5	LX4 *Δald6*	This study
LX6	LX5 *ald6Δ::P$_{TEF2}$-CDC19-T$_{CYC1}$*	This study

#216120), YIP_BC02 (Addgene #216121)*,* and YIP_BC03 (Addgene #216122). All genetic modifications were introduced using CRISPR/Cas9-mediated genome editing as preciously described (Camara et al., 2020), i.e., the dummy of pYN2_1 was replaced with sgRNA fragments ordered as oligonucleotides. PCR products amplified from plasmids YIP_BC01-BC03 were purified with the GeneJET PCR purification kit (Thermo Fisher Scientific, USA) and co-transformed (Gietz and Schiestl, 2007) with plasmids BC01–05 containing sgRNA sequences designed by CRISPR-ERA (Liu and Wang, 2021). The replacement of *CYB2*, and *GPD1* was achieved by integration of the PCR-amplified *LDH* expression cassette of YIP_BC01, whereas *ERF2* was replaced by *LDH* amplified from YIP_BC02. The PCR primers contained 40 bp homologous sequences flanking the targeted gene. The resulting strain was named LX3 and has six copies of *LDH* integrated in the genome (Table 1). The deletion of *PHO13* and *ALD6* from LX3 was achieved with oligonucleotide cassettes containing 40 bp homologous sequences flanking the targeted gene locus, resulting in strains LX4 and LX5, respectively. Finally, the *CDC19* cassette was PCR amplified from YIP_BC03 with primers containing 40 bp homologous sequences flanking *ADL6*. This final strain, LX6, has *ALD6* replaced by an additional copy of the endogenous *CDC19* gene, expressed under the strong *TEF2* promoter. All strains were confirmed by PCR. Oligonucleotide synthesis and Sanger sequencing of PCR products and plasmids was done by Eurofins genomics (Eurofins, Luxembourg). All plasmids and primers used for strain construction can be found in Supplementary Tables S1 and S2. *Escherichia coli* Top 10 cells were used for construction and propagation of plasmids. *E. coli* cells were cultivated in Luria broth supplemented with 100 μg/L ampicillin.

2.3. Fermentation in microtiter plates and shaking flasks

Yeast precultures were inoculated from solid medium cultures, grown overnight in 3 mL YPD (20 g/L glucose), YPX (20 g/L xylose), or SLH medium in 14 mL culture tubes before cells were collected, washed with sterilized water, and used for inoculation. Shaking flask cultures of 40 mL (in 250 mL Erlenmeyer flasks) and microtiter fermentation in 96-well plates where each well contained 250 μL YP medium with various glucose and xylose concentration or SLH medium were inoculated at initial optical density at 600 nm (OD$_{600}$) of 0.1. The Erlenmeyer flasks were shaken at 200 rpm in an Innova 44 shaker (Eppendorf, Germany) whereas the 96-well plates were shaken at 250 rpm in a Growth profiler 960 device (Enzyscreen, Netherlands). For studying the effect of oxygen-limitation, cultures with 10 mL medium shaking at 250 rpm were compared to cultures with 30 mL medium shaking at 150 rpm, using 50 mL Erlenmeyer flasks. All the yeast cultures were carried out at 30 °C and all experiments were repeated independently in triplicate.

For the microtiter fermentation, the growth data was collected as green values and converted to OD$_{600}$ based on a standard curve, following the instructions of the Growth Profiler (Enzyscreen, Netherlands). Cell growth in flask fermentation was monitored by measuring the OD$_{600}$ on a GENESYS 10 UV–Vis spectrophotometer (Thermo Scientific, USA). The biomass concentration in flask fermentation with CaCO$_3$ was determined by measuring the OD$_{600}$. The remaining CaCO$_3$ in the culture broth was dissolved by addition of 600

μL of 0.5 M phosphoric acid (85 %, Sigma Aldrich, USA) according to Yang et al. (2015).

2.4. Bioreactor fermentations

Cells of 100 mL precultures grown in 500 mL Erlenmeyer flasks at 30 °C, shaking at 200 rpm were harvested at mid-exponential phase (at an OD$_{600}$ of approx. 4) and washed with sterilized water before being used for bioreactor inoculation. Batch fermentations were performed at 30 °C, at pH 6.0, and with a dissolved oxygen (DO) level >30 % in 2.5 L Biobench bioreactors (Biostream International BV, the Netherlands) containing 1 L of modified SLH medium. The DO level was maintained by automatically increasing the agitation rate from 300 to 900 rpm and supplying microfiltrated (0.22 μm) air at a flow rate of 1.0 vol/vol/min (vvm). The pH was controlled by the automatic addition of 8 % (v/v) NH$_4$OH and 2 N HCl solutions. Culture samples were collected every 3 h with at least 3 replicates.

2.5. Metabolic modeling

The yeast consensus genome-scale model (Lu et al., 2019) version 8.6.2 (Sánchez et al., 2018) was expanded to an enzyme-constrained model (ecYeast) using GECKO v3. Subsequently, a strain-specific model for CEN.PK XXX was created by incorporation of the reactions mediated by D-xylose reductase (UniProt: P31867), D-xylulose reductase (UniProt: P22144) from *S. stipites*, and L-lactate dehydrogenase (UniProt: P19858) from *B. taurus* (Table 2) to allow xylose utilization. Additionally, the lactate exchange reaction (r_1207) was set to be reversible to allow lactic acid production. Strain specific models were constructed for LX3, LX4, and LX5. Then, metabolic targets were predicted using Flux Scanning based on Enforced Objective Flux (FSEOF) (Choi et al., 2010) in GECKO v3, at 1 and 10 mmol/gDCW/h uptake rate to avoid inducing the Crabtree Effect. This method scans and selects all the metabolic fluxes that (i) increase or (ii) decrease product formation in the ecModel after enforcing the objective target. This introduces an additional constraint during flux analysis and is repeated in n steps between the 90% of the maximum and minimum theoretical yield. Then for selected fluxes a slope is calculated as the difference in the flux when the enforced objective target production is set to 90% of the maximum theoretical yield and the flux when the enforced objective target production is set to the minimum for the reaction *j*, divided by maxTarget-maxTarget/nSteps-1.

$$slope = \frac{abs(v_{n-1} - v_1)_j}{\max Yield - \frac{\max Yield}{n-1}}$$

Where *v* is the flux for the reaction *j*. MaxYield is 90% of the maximum theoretical yield for the target. *N* is the number of steps that lactic acid production is enforced through.

Gene knockouts were simulated by setting upper and lower bounds of the respective protein usage reaction to zero. To induce a flux through the Pentose Phosphate Pathway based on previously observed xylose utilization patterns (Eglinton et al., 2002; Westman et al., 2014), which represents overexpressed genes *RPE1, TAL1,* and *RKI1* in CEN.PK XXX (Table 1), the minimum usage of these proteins was constrained at 5% of their maximum allowable usage. The maximum allowable usage itself

Table 2
New reactions incorporated to the yeast ecModel.

Gene	Enzyme	Reaction	k_{cat}	Reference
XYL1_PICST	P31867	D-xylose + NADPH + H+ => xylitol + NADP (+)	27.5	Liang et al. (2007)
XYL2_PICST	P22144	xylitol + NAD => D-xylulose + NADH + H+	17.5	Watanabe et al. (2005)
LDHA_BOVIN	P19858	H+ + NADH + pyruvate => (S)-lactate + NAD	3.11	Tokuhiro et al. (2009)

was determined through a Flux Variability Analysis (FVA) conducted at 1 mmol/gDCW/h glucose. For *in silico* implementation of targets predicted by ecFSEOF, the corresponding enzyme usage reactions were constrained to either zero (i.e., knockout), an increased minimum amount of protein usage (i.e., overexpression), or a decreased maximum amount of protein usage (i.e., knockdown). All simulations were carried out in MATLAB R2023b with Gurobi 10.0.3 as solver in the RAVEN toolbox (Wang et al., 2018). The source code used in this study is available at: https://doi.org/10.5281/zenodo.10391081.

2.6. Analytical methods

Culture supernatants were filtrated with 0.45 μm syringe filters and analyzed using high performance liquid chromatography (HPLC). The concentration of L-lactic acid, xylose, glucose, acetic acid, and ethanol in YPD and YPX media was determined using a Dionex UltiMate 3000 series HPLC (ThermoFisher Scientific, USA) equipped with a Dionex RI-101 refractive index detector and an Aminex HPX-87H column (7.8 × 300 mm, Bio-Rad, USA) operating at 50 °C and 0.7 mL/min of a flow rate with 5 mM H_2SO_4 as an isocratic mobile phase. Since the chromatograms of mannose and galactose could not be separated with the Aminex HPX-87H column, glucose, xylose, mannose, galactose, and arabinose were quantified as a mixed solution and are for simplicity referred to as "sugars". For quantification of furfural and HMF used for the SLH medium, standard curves of each component were prepared and detected with a Dionex VWD-3400 R S variable wavelength detector and Rezex RFQ-Fast Acid H^+ (8 %) ion exclusion column (7.8 × 100 mm, Phenomenex, USA) maintained at 80 °C at a flow rate of 0.6 mL/min using 5 mM H_2SO_4 as the isocratic mobile phase. Furfural and HMF were observed at 276 nm and 284 nm, respectively.

2.7. Statistical analysis

Statistical analyses were performed in SigmaPlot 12.0 (Systat Software Inc., USA). The differences between the strains in terms of metabolite production and consumption were tested by a two-tailed *t*-test. Statistical significance was established at $p < 0.05$ and marked by × $p < 0.05$, **$p < 0.01$, and ***$p < 0.001$.

3. Results and discussion

3.1. Construction and characterization of the initial lactic acid producing strain

A lactic acid producing strain was constructed by introducing multiple *LDH* genes while deleting *CYB2, ERF2,* and *GPD1* in a diploid xylose

fermenting strain, CEN.PK XXX (Westman et al., 2014). The deletion of *CYB2* was previously shown to prevent assimilation of lactate at low pH (Ookubo et al., 2008) while the deletion of *ERF2*, encoding an acyl-transferase involved in protein palmitoylation, was shown to increase lactic acid production from glucose (Baek et al., 2017). Similarly, deletion of the glycerol pathway genes *GPD1* and *GPD2* was demonstrated to improve lactic acid production from glucose (Baek et al., 2016). Noteworthy, the deletion of both these genes was shown to lead to poor growth due to unbalanced redox regulation and high osmosensitivity (Ansell et al., 1997). Hence, we deleted only *GPD1*, as Gpd1 is responsible for the majority of the glycerol produced (Remize et al., 2003). The resulting strain, LX3, with six copies of the *LDH* gene integrated at *CYB2, ERF2,* and *GPD1*, produced 10.7 ± 0.4 g lactic acid/L from 50 g/L of glucose within 30 h (Fig. 1b). A cell density of $OD_{600} = 9.5$ was reached at the point of maximum lactic acid concentration (Fig. 1a). The yield of LX3 was 0.21 g lactic acid/g glucose at a productivity of 0.36 g lactic acid/L/h. Notably, the lactic acid yield of LX3 that is PDC-positive, was similar to what was previously shown with *S. cerevisiae* engineered for *PDC1* inactivation (Table 3), e.g., 0.18 g/g glucose (Novy et al., 2018) or 0.26 g/g glucose (Colombié et al., 2003). Ethanol was still the major product of LX3, reaching 14.9 ± 0.3 g/L with a yield of 0.31 g ethanol/g glucose consumed and a productivity of 0.49 g ethanol/L/h. Lane et al. (2023) reasoned that the Crabtree effect leads to the glycolytic flux to ethanol being dominant over the flux to lactic acid in a PDC-positive strain.

In YPX medium with 50 g/L xylose, LX3 produced 30.3 ± 0.3 g lactic acid/L within 41 h (Fig. 1b). The yield and productivity of lactic acid from xylose were 0.61 g lactic acid/g xylose and 0.73 g lactic acid/L/h, respectively. Thus, the LX3 strain produced three times more lactic acid from xylose compared to the production from glucose. Whereas all glucose was utilized within 30 h, 18 g/L of xylose remained after 41 h. At this time point, the pH of the medium had decreased to 3.5 from the initial pH of 6.8. The pKa of lactic acid is 3.8 and at a pH below that, the predominantly undissociated and uncharged lactic acid will transverse the plasma membrane. The accumulated lactic acid cannot freely diffuse out of the cells that aim to maintain a neutral cytosolic pH, which can cause severe problems such as inhibition of membrane trafficking (Bauer et al., 2003), intracellular acidification (Viegas et al., 1998), and ATP depletion (Piper et al., 2001). Intracellular acidification has been reported to disrupt glycolysis in *S. cerevisiae* (Imai and Ohno, 1995; Krebs et al., 1983), which may explain why the LX3 cells failed to use all xylose provided.

In LX3 cultures grown in YPX medium, merely 1.6 ± 0.4 g/L of ethanol was detected (Fig. 1b) and the cell density was lower compared to cultivation on glucose, reaching an OD_{600} of 5.8 after 41 h (Fig. 1a). The lactic acid yield on xylose of LX3 was 0.61 g lactic acid/g xylose,
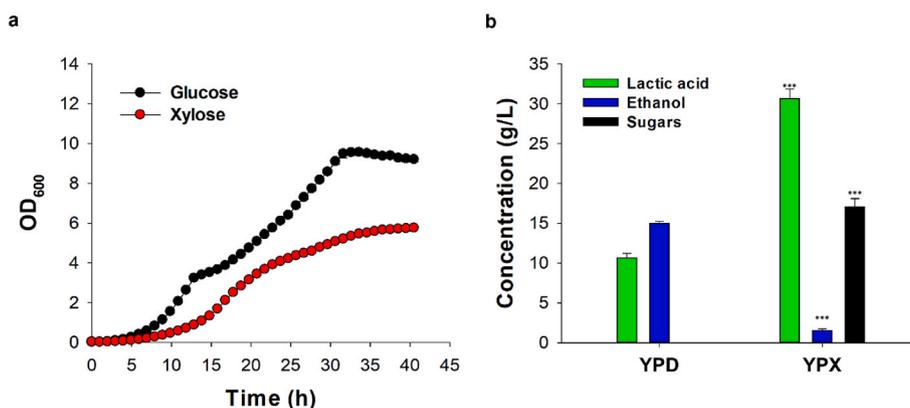

Fig. 1. (a) Growth profiles and (b) titers of lactic acid (green) and ethanol (blue) produced by LX3 after 144 h with 50 g/L glucose in YPD medium or 50 g/L xylose in YPX medium. Any residual glucose or xylose are marked in black. Values shown are the means of three independent experiments, and the error bars indicate the standard error. A two-tailed *t*-test was used for statistical analysis, *** indicates $p < 0.001$.

Table 3
Examples of lactic production by various engineered *S. cerevisiae* strains.

LDH Origin	Produc-tivity (g/L/h)	Titer (g/L)	Yield (g/g)	Carbon source[a]	Buffering agent	Reference
Leuconostoc mesenteroides	2.20	112	0.80	glc	50 g/L CaCO₃	Baek et al. (2016)
B. taurus	2.54	122	0.61	glc, suc	1 N NaOH	Saitoh et al. (2005)
P. sinensis, B. taurus	3.55	142	0.89	glc	5 N Ca(OH)₂	Song et al. (2016)
Lactobacillus plantarum	1.00	70	0.93	glc	4.5 g/L CaCO₃	Valli et al. (2006)
Lactococcus lactis, Bacillus coagulans	1.68	192	0.78	glc	65 g/L CaCO₃	Liu et al. (2023)
Lactobacillus acidophilus	1.24	119	0.72	glc	–	Jang et al. (2021)
B. taurus	0.43	82	0.81	glc	30 g/L CaCO₃	Ishida et al. (2006b)
B. taurus	1.54	74	0.69	glc	8 M NaOH	Tokuhiro et al. (2009)
R. oryzae	0.47	49	0.60	xyl	10 N NaOH	Turner et al. (2015)
R. oryzae	0.42	83	0.66	glc, xyl, cel	50 g/L CaCO₃	Turner et al. (2016)
L. mesenteroides	1.35	65	0.26	LH; glc, xyl	28 g/L CaCO₃	Lam et al. (2021)
B. taurus	0.73	30	0.61	xyl	–	This study
B. taurus	0.78	93	0.84	xyl	40 g/L CaCO₃	This study
B. taurus	0.21	30	0.75	SLH; glc, xyl, gal, man	20 g/L CaCO₃	This study

[a] glc = glucose, suc = sucrose, xyl = xylose, cel = cellobiose, gal = galactose, man = mannose, LH = lignocellulosic hydrolysate, SLH = synthetic lignocellulosic hydrolysate.

superior to what was previously reported for *S. cerevisiae* SR8 expressing *ldhA* from *Rhizopus oryzae* when grown in medium with 40 g/L xylose, lacking a neutralizing agent; 0.48 g lactic acid/g xylose (Turner et al., 2015). Like LX3, the SR8 strain predominantly produced ethanol when grown on glucose. Turner et al. (2015) suggested that the slower uptake of xylose compared to that of glucose results in a lower intracellular pyruvate concentration, which can allow for the LDH to rapidly convert pyruvate to lactic acid, before the pyruvate concentration is high enough to favor conversion to ethanol.

3.2. Characterization of lactic acid production at high concentrations of xylose

The reaction between CaCO₃ and lactic acid leads to formation of calcium lactate and neutralization of the pH in the range of pH 5–7 (Hetényi et al., 2011). An enhanced xylose utilization and lactic acid yield through pH buffering was observed previously (Turner et al., 2015; Baek et al., 2016). Therefore, the LX3 strain was cultivated in YPX medium with ~50 g/L xylose, and 20 g/L CaCO₃. In this setup, the LX3 stain produced 43.8 ± 1.7 g/L of lactic acid from 53 g/L of xylose within 55 h (Fig. 2a, Table 4). The yield and productivity were 0.75 g lactic acid/g xylose consumed and 0.80 g lactic acid/L/h, respectively. Remarkably, the ethanol accumulation was negligible. The pH of the medium decreased sharply from 6.8 to 5.4 after the produced lactic acid exceeded 1 g/L but remained at pH 5.6 until the end of the fermentation (data not shown). When the LX3 strain was cultivated in YPX medium with increasing concentrations of xylose (40, 60, 90, and 110 g/L) and CaCO₃ (20–30 g/L), all xylose was consumed within 120 h (Fig. 2b). The

Table 4
Lactic acid production by the LX3 strain in YPX medium with various concentration of xylose, buffered with CaCO₃, n = 3. Values represent means ± standard errors.

Xylose concentration (g/L)	Titer (g/L)	Yield (g lactic acid/ g xylose)	Productivity (g lactic acid/L/h)
40.3 ± 1.2	26.2 ± 3.5	0.73	0.73
61.5 ± 0.7	40.4 ± 1.7	0.77	0.79
88.8 ± 3.4	72.9 ± 1.2	0.82	0.86
110.5 ± 1.6	93.0 ± 3.1	0.84	0.78

lactic acid concentration reached up to 93.0 ± 3.1 g/L with 110.5 g/L of xylose being utilized at 120 h. The highest yield of 0.84 g lactic acid/g xylose consumed, and a productivity of 0.78 g lactic acid/L/h were achieved in cultures with 110 g/L xylose (Table 2). To the best of our knowledge, this presents the highest lactic acid titer and yield from xylose fermentation reported thus far. The final concentration of ethanol remained below 1 g/L at all xylose concentrations tested, demonstrating that xylose conversion to lactic acid can be achieved without disturbing the metabolic pathway for ethanol production, which is commonly done when lactic acid is produced from glucose (Dai et al., 2018). The strong tendency for pyruvate originating from xylose to become converted into lactic acid is not yet completely understood but may be connected with glucose signaling and metabolism playing a central role in flux
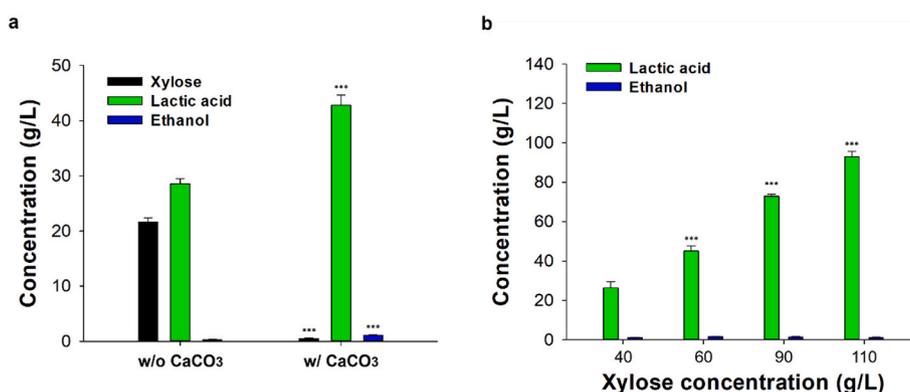

Fig. 2. (a) Titers of lactic acid (green) and ethanol (blue) produced with the LX3 after 50 h in YPX medium with 50 g/L xylose without buffering or buffered with 20 g/L CaCO₃ or (b) in buffered YPX medium with various concentration of xylose after 36 h (40 g/L), 60 h (60 g/L), 84 h (90 g/L), 120 h (110 g/L) of fermentation. Any residual xylose is marked in black. Values shown are the means of three independent experiments, and the error bars indicate the standard error. A two-tailed *t*-test was used for statistical analysis; *** indicates *p* < 0.001.

distribution at the pyruvate branch point (Lane et al., 2023).

3.3. Optimization of lactic acid production from xylose

For effective fermentation of lignocellulosic biomass, the strain needs to be robust against harsh conditions such as presence of toxic inhibitors in the fermentation medium. Many successful evolutionary engineering attempts as well as a great number of genetic alterations leading to increased tolerance to inhibitors in lignocellulosic hydrolysates have been reported (Camara et al., 2022). One targeted engineering example is deletion of *PHO13* that was reported to lead to high tolerance to fermentation inhibitors such as acetic acid, formic acid, and furfural (Fujitomi et al., 2012; Li et al., 2014) and to improve pentose assimilation (Ni et al., 2007; Van Vleet et al., 2008; Ye et al., 2019).

Therefore, to increase lactic acid production and enable lactic acid production in the SLH medium, *PHO13* was deleted from LX3, resulting in LX4. The LX4 strain had a 1.1-fold higher lactic acid titer (30.9 $\pm$ 1.6 g/L) compared to the LX3 strain (27.9 $\pm$ 1.9 g/L) in YPX medium with 40 g/L xylose (Fig. 3a). Similarly, from the total of 40 g/L of sugars (glucose, xylose, galactose, and mannose), LX4 produced 24.5 $\pm$ 1.3 g/L of lactic acid, that was 1.1-fold higher compared to the titer of LX3 (21.9 $\pm$ 2.3 g/L, Fig. 3b). Still, neither strain consumed all of the sugars of the SLH medium, as approx. 2 g/L of sugars, presumably xylose, remained after 144 h of fermentation (Fig. 3b).

Kim et al. (2013) reported that the lag time of a *PHO13* negative strain in medium with 40 g/L of xylose decreased from 24 h to 10 h. In line with this, Van Vleet et al. (2008) had observed up to 10 times increased growth and xylose consumption rates upon deletion of *PHO13*.
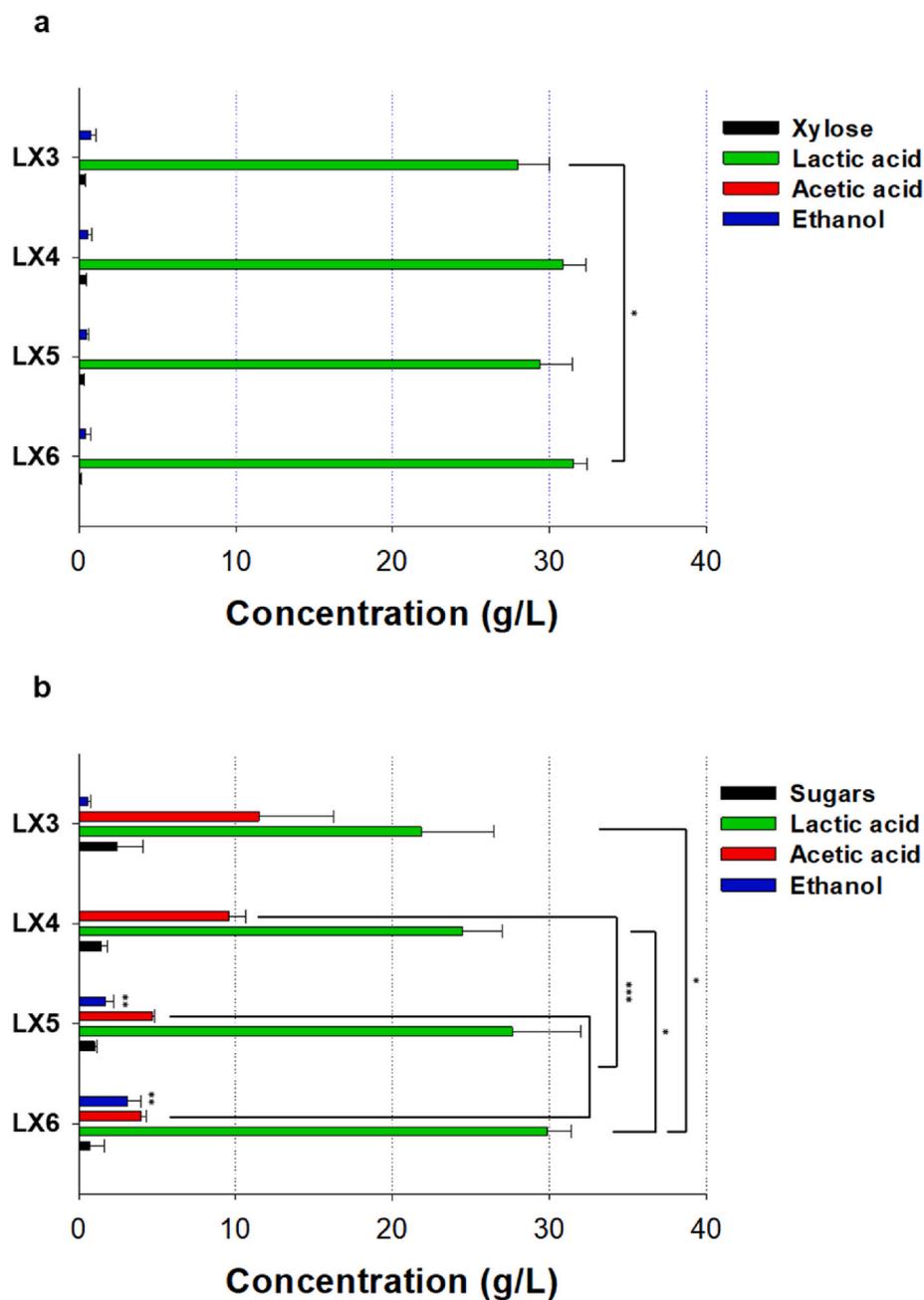

Fig. 3. Titers of lactic acid (green), ethanol (blue), and acetic acid (red) produced by LX3, LX4, LX5, and LX6 after 144 h in CaCO$_3$ (20 g/L) buffered (a) YPX medium with 40 g/L xylose or (b) SLH medium, after 144 h of fermentation. Any residual xylose or sugars (xylose, galactose, and mannose) are marked in black. Values shown are the means of three independent experiments, and the error bars indicate the standard error. A two-tailed *t*-test was used for statistical analysis; * indicates $p < 0.05$, ** $p < 0.01$, and *** $p < 0.001$.

Nonetheless, in our study, no significant difference in biomass and xylose consumption between LX4 and LX3 was observed when xylose was the sole carbon source (Supplementary Fig. S2). The role of Pho13 has not been elucidated but it has been suggested that Pho13 activity may generate a futile cycle by dephosphorylating xylulose-5-phosphate, resulting in an accelerated ATP depletion and flux blockage (Kim et al., 2013). Van Vleet et al. (2008) observed a 10-fold decrease in glycerol production from xylose upon deletion of *PHO13*. They hypothesized that lower glycerol production could indicate that less excess NADH was produced by the *Δpho13* mutant during assimilation of xylose. In line with this, 12 differentially expressed genes were noted for a *Δpho13* mutant grown on glucose whereas 277 differentially expressed genes were identified when the strain was grown xylose (Kim et al., 2015). Among them, 9 genes upregulated in both conditions were directly or indirectly involved in NADPH regeneration; pentose phosphate pathway genes (*GND1*, *SOL3*, and *TAL1*), NADPH specific oxidoreductase encoding genes (*CGY1* and *GOR1*), and a NADH kinase encoding gene (*TEF1*) (Kim et al., 2015). Moreover, a metabolomics study reported a 98 % reduction in sedoheptulose content of a *Δpho13* mutant (Xu et al., 2016). At the non-oxidative phase of the pentose phosphate pathway, sedoheptulose-7-phosephate and glyceraldehyde-3-phosphate are turned into erythrose 4-phosphate are fructose 6-phosphate by trans-aldolases. Xu et al. (2016) suggested that dephosphorylation of sedoheptulose-7-phosphate and accumulation of sedoheptulose in strains with intact *PHO13* might cause limited transaldolase activity, leading to inefficient xylose metabolism. This could perhaps also be a reason for the increased lactic acid production of LX4 lacking *PHO13*.

3.4. Deletion of ALD6 for preventing acetate accumulation

Acetic acid is produced as a by-product during alcoholic fermentation, and it can be used as a carbon source while even relatively low concentrations acetic acid are inhibitory to *S. cerevisiae* (Guaragnella and Bettiga, 2021). Acetic acid formed during hydrolysis of acetyl groups of hemicelluloses during the pretreatment is often found in rather high amounts in lignocellulosic hydrolysates (up to 11.5 g/L; Vanmarcke et al., 2021). While no acetic acid was observed for LX3 and LX4 in YPX medium (Fig. 3a), both strains produced and accumulated acetic acid during the cultivation in SLH medium that contained 2.6 g/L of acetic acid. The final titer of acetic acid was 11.5 ± 2.0 g/L and 9.6 ± 1.2 g/L after 144 h of fermentation by LX3 or LX4, respectively (Fig. 3b). As deletion of *ALD6*, encoding an aldehyde dehydrogenase, was previously shown to reduce acetate production (Eglinton et al., 2002; Kim et al., 2013), we deleted *ALD6* from LX4, resulting in LX5. In YPX, the lactic acid titer of LX5 was similar to that of its LX4 strain, 29.4 ± 2.2 g/L (Fig. 3a) but in SLH medium the LX5 strain produced 27.7 ± 1.9 g lactic acid/L compared to 24.4 ± 1.7 g lactic acid/L produced by LX4 (Fig. 3b), a 1.1-fold increase in lactic acid production. The acetic acid accumulation of LX5 was reduced to 4.7 ± 0.2 g/L, a 2-fold decrease compared to the LX4 strain that produced 9.6 ± 1.2 g acetate/L in the SLH medium (Fig. 3b). Notably, the deletion of *ALD6* also resulted in ethanol accumulation, as 1.7 ± 0.8 g/L ethanol remained in the SLH medium after 144 h of cultivation (Fig. 3b). Both acetic acid and ethanol are produced from acetaldehyde though a single reaction, by alcohol dehydrogenases converting acetaldehyde into ethanol or aldehyde dehydrogenases turning acetaldehyde into acetic acid. When the metabolic flux into the acetic acid is depressed, the flux towards ethanol synthesis can be expected to be stronger, as already suggested by Papapetridis et al. (2016).

3.5. Metabolic modeling for increasing the lactic acid production

To further increase the lactic acid production rate (and yield) by *S. cerevisiae*, FSEOF in GECKO (ecFSEOF) was used to predict metabolic engineering targets using constructed strain-specific models for CEN.PK XXX, LX3, LX4 and LX5. To improve interpretability of the modeling results and reflect the experimental data showing that *S. cerevisiae*

sequentially consumed xylose and glucose (Fig. S1), simulations were performed separately for glucose and xylose. The results from the ecF-SEOF analysis suggested a total of 226 unique gene targets that could increase lactic acid production during glucose and xylose utilization. Targets predicted included overexpression of *XKS1*, LDHA_BOVIN, *TAL1*, *XYL2*, *XYL1*, *RKI1*, and *RPE1*, as well as knockout of *CYB2* and knockdown of *ALD6*, all of which were already experimentally overexpressed/knockout (Table 1, Fig. 4b). *Per se*, this "validation" showcases the predictive power of the constrained enzyme model.

While flux balance analysis returns unique flux distributions, in reality the models represent larger solution spaces that can meet the growth and lactic acid production demands to different degrees. To confirm and select potential gene targets, the minimum and maximum lactic production rate was determined after fixing the enzyme usage for each predicted protein target individually, in accordance with the type of predicted genetic intervention (i.e., overexpression, knockdown, knockout) and setting the growth rate to 25% of the maximum rate predicted. The maximum and minimum theoretical production rates were calculated by minimizing or maximizing the specified product, as comparing these could indicate a high uncertainty in the production that the yeast would perform *in vivo*. Fig. 4 shows the prioritized targets that ecFSEOF predicted for overexpression. While *TDH3* was suggested as promising target to increase lactic production, this is likely an artefact of its ecModel-incorporated *in vitro* k_{cat} value being a significant underestimation of its *in vivo* k_{cat}, as has previously been observed (Dinh and Maranas, 2023). Instead, *CDC19* was deemed as the most promising target for experimental validation to increase lactic acid production from both glucose and xylose (Fig. 4). Therefore, based on the modeling, we constructed LX6 to overexpress *CDC19*. LX6 produced 31.5 ± 1.1 g/L lactic acid in YPX medium and 29.9 ± 1.4 g/L of lactic acid in the SLH medium. In YPX medium, the lactic acid titer was similar for LX3, LX4, LX5 and LX6. In SLH medium the LX6 strain produced significantly more lactic acid and 2.9 times less acetic acid (4.0 ± 0.3 g/L) when compared to LX3. Compared to LX5 there was no significant differences in lactic acid production, but LX6 produced 1.8 times more ethanol (3.1 ± 0.3 g/L) (Fig. 4). This is likely due to overexpression of *CDC19* leading to accelerated pyruvate accumulation. The yield of lactic acid of LX6 (0.75 g/g) from a lignocellulosic hydrolysate mimicking medium is the highest noted so far.

3.6. Lactic acid production under oxygen-limited condition

Production of lactic acid from xylose has been described to increase under oxygen-limited conditions (Novy et al., 2018). Therefore, the LX5 strain was grown under oxygen-limitation, in either YPX medium with 40 g/L xylose or SLH medium, both buffered with 20 g/L CaCO₃. Expectedly, more (1.3-fold) lactic acid was produced in YPX medium with limited oxygen supply compared to the fully aerobic condition (37.0 ± 1.9 g/L vs. 28.9 ± 0.3 g/L, Fig. 5a). On the contrary, 1.3 times less lactic acid was produced in SLH medium with oxygen limitation compared to the fully aerobic condition (19.2 ± 2.1 g/L vs. 24.5 ± 1.3 g/L).

To investigate the link between oxygen-limitation and lactic acid production, we used metabolic modeling and gene essentiality as predicted by the ecModel, while forcing lactic acid production to be at 90% of the predicted maximum theoretical yield. This analysis should identify genes that are essential for supporting growth during high lactic acid production. Remarkably, all essential genes in glucose (53 genes) were also predicted as essential for growth in xylose. In addition, 38 genes were predicted to be essential for production from xylose, including a total of twenty genes that encode proteins that are part of the mitochondrial respiratory chain complex III and IV (Supplementary Table S3). Notably, the protein usage of these complexes showed a negative correlation with lactic acid production (determined by ecF-SEOF), suggesting these genes as knockdown targets. As such, for increased lactic acid production, it appears beneficial to reduce the flux
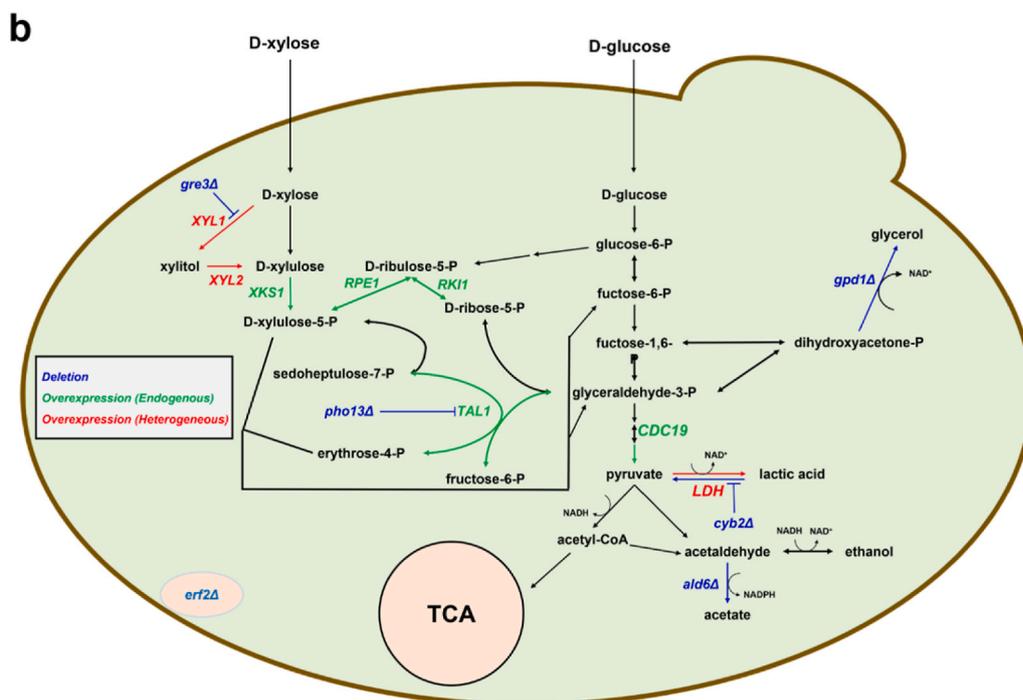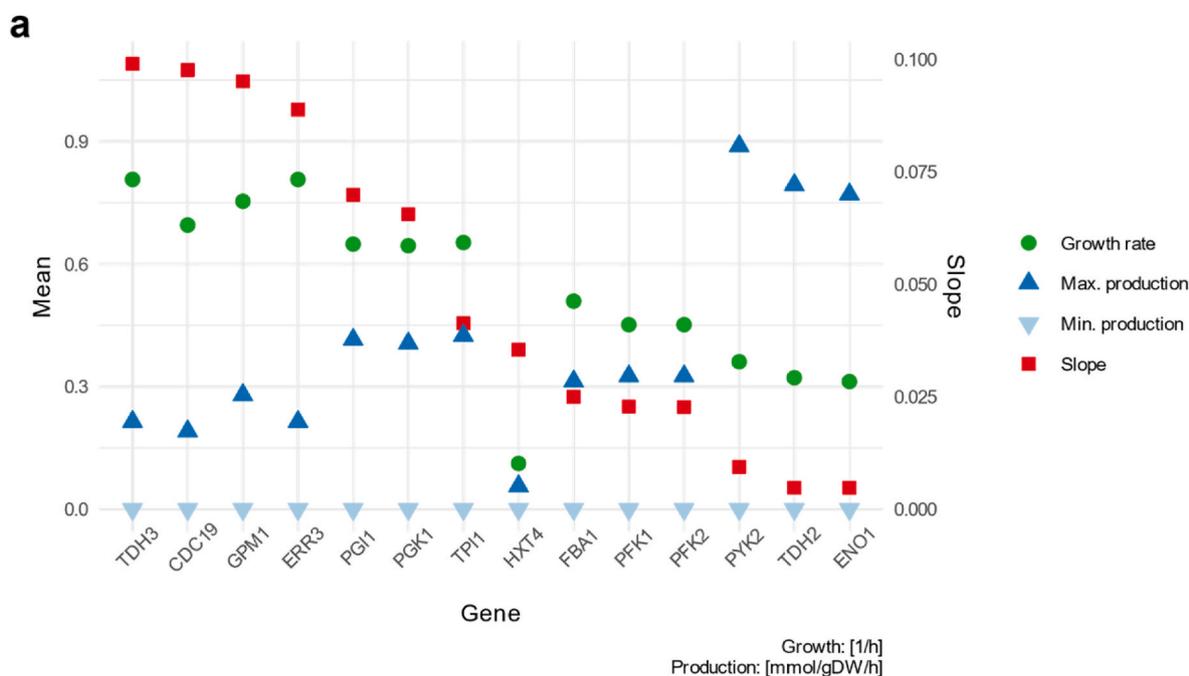
Fig. 4. (a) Targets to be overexpressed, as predicted by ecFSEOF. The slope is an ecFSEOF-derived score that represents how strongly the gene target correlates with product formation. The indicated minimum and maximum product formation are model predictions where overexpression of the indicated protein is implemented by increasing the lower constraint in its usage reaction. (b) Overview of the metabolic pathway for utilization of xylose and production of lactic acid in LX6: red arrows indicate overexpression of heterogeneous genes; green arrows overexpression of endogenous genes and blue arrows deletion of genes.

through the oxidative phosphorylation pathway. This is in concordance with previous observations on oxygen availability playing an important role in xylose utilization and ethanol and xylitol production (Jin and Jeffries, 2004). This is likely due to demand for oxygen-requiring respiration to regenerate NAD used by the xylose dehydrogenase (Maas et al., 2008) and ATP depletion at high respiratory rates induced

by the xylulokinase that catalyzes the ATP-dependent conversion of xylulose into xylulose 5-phosphate (Jin et al., 2003). We hypothesize that the active oxidative phosphorylation in the aerobic YPX cultivation might result in accumulation of toxic xylulose 5-phosphate (Jin et al., 2003). Lower ATP production during oxygen-limitation can be expected to limit the xylulose 5-phosphate levels in the cells, leading to less ATP
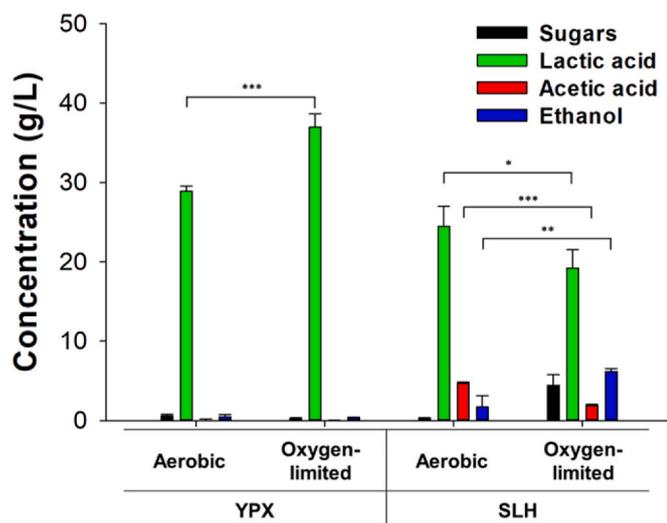
Fig. 5. Titers of, lactic acid (green), ethanol (blue), and acetic acid (red) of LX5 after 144 h, in YPX medium with 40 g/L xylose in or in SLH medium, both media buffered with 20 g/L CaCO$_3$. Any residual xylose or sugars are marked in black. The values shown are the means of three independent experiments, and the error bars indicate the standard deviations. A two-tailed *t*-test was used for statistical analysis, * indicates $p < 0.05$, **$p < 0.01$ and ***$p < 0.001$.

available for essential activities (Jin et al., 2003). In order for the cells to detoxify and tolerate the inhibitors, they demand more ATP (Jonsson et al., 2013) which could explain the reduced lactic acid production in the oxygen-limitation SLH medium. Notably, 2.5 times more acetic acid was produced in the fully aerobic SLH cultures (4.7 g/L) compared to the oxygen limited cultures (1.9 g/L, Fig. S2). Higher levels of acetic acid are known to be produced by cells under aerobic conditions compared to anaerobic fermentation (Curiel et al., 2016). NADP$^+$-dependent decarboxylation of pyruvate to acetaldehyde that can be oxidized to acetic acid, is an intermediary step towards ethanol production.

4. Conclusions

Rational strain engineering combined with model-based strain optimization was employed for efficient production of lactic acid from lignocellulosic hydrolysates containing multiple carbon sources and inhibiting compounds such as acetic acid. A yield of 0.75 g lactic acid/g sugar consumed was reached with LX6 in a synthetic lignocellulosic hydrolysate medium. In YPX medium, a production of 93 g/L of lactic acid and a yield of 0.85 g lactic acid/g xylose consumed was reached. Furthermore, model-based prediction for lactic acid production in oxygen-limited compared to fully aerobic conditions gave novel insights into the role of oxygen in lactic acid production from xylose or SLH medium. Whereas xylose production at oxygen-limitation may be increased by a reduced flux through the oxidative phosphorylation pathway, higher oxygen levels may lead to higher ATP concentrations that are needed for tolerating the inhibitors of the SLH medium. The work demonstrates the potential for lactic acid production with *S. cerevisiae* strains lacking alterations in modification of the ethanol metabolism and highlights the feasibility of lactic acid production from renewable feedstocks such as lignocellulosic hydrolysates.

CRediT authorship contribution statement

Bohyun Choi: Writing – original draft, Visualization, Methodology, Investigation, Formal analysis. **Albert Tafur Rangel:** Writing – original draft, Software, Methodology, Investigation, Formal analysis. **Eduard J. Kerkhoven:** Writing – review & editing, Supervision, Conceptualization. **Yvonne Nygård:** Writing – review & editing, Supervision, Funding

acquisition, Conceptualization.

References

Ansell, R., Granath, K., Hohmann, S., Thevelein, J.M., Adler, L., 1997. The two isoenzymes for yeast NAD(+)-dependent glycerol 3-phosphate dehydrogenase encoded by *GPD1* and *GPD2* have distinct roles in osmoadaptation and redox regulation. EMBO J. 16 (9), 2179–2187. https://doi.org/10.1093/emboj/16.9.2179.

Baek, S.H., Kwon, E.Y., Bae, S.J., Cho, B.R., Kim, S.Y., Hahn, J.S., 2017. Improvement of d-lactic acid production in *Saccharomyces cerevisiae* under acidic conditions by evolutionary and rational metabolic engineering. Biotechnol. J. 12 (10) https://doi.org/10.1002/biot.201700015.

Baek, S.H., Kwon, E.Y., Kim, Y.H., Hahn, J.S., 2016. Metabolic engineering and adaptive evolution for efficient production of D-lactic acid in *Saccharomyces cerevisiae*. Appl. Microbiol. Biotechnol. 100 (6), 2737–2748. https://doi.org/10.1007/s00253-015-7174-0.

Bamba, T., Hasunuma, T., Kondo, A., 2016. Disruption of *PHO13* improves ethanol production via the xylose isomerase pathway. Amb. Express 6 (1), 4. https://doi.org/10.1186/s13568-015-0175-7.

Bauer, B.E., Rossington, D., Mollapour, M., Mamnun, Y., Kuchler, K., Piper, P.W., 2003. Weak organic acid stress inhibits aromatic amino acid uptake by yeast, causing a strong influence of amino acid auxotrophies on the phenotypes of membrane transporter mutants. Eur. J. Biochem. 270 (15), 3189–3195. https://doi.org/10.1046/j.1432-1033.2003.03701.x.

Burgard, A.P., Pharkya, P., Maranas, C.D., 2003. Optknock: a bilevel programming framework for identifying gene knockout strategies for microbial strain optimization. Biotechnol. Bioeng. 84 (6), 647–657. https://doi.org/10.1002/bit.10803.

Camara, E., Lenitz, I., Nygård, Y., 2020. A CRISPR activation and interference toolkit for industrial *Saccharomyces cerevisiae* strain KE6-12. Sci. Rep. 10 (1), 14605 https://doi.org/10.1038/s41598-020-71648-w.

Camara, E., Olsson, L., Zrimec, J., Zelezniak, A., Geijer, C., Nygård, Y., 2022. Data mining of *Saccharomyces cerevisiae* mutants engineered for increased tolerance towards inhibitors in lignocellulosic hydrolysates. Biotechnol. Adv. 57, 107947 https://doi.org/10.1016/j.biotechadv.2022.107947.

Chen, Y., Gustafsson, J., Tafur Rangel, A., Anton, M., Domenzain, I., Kittikunapong, C., Li, F., Yuan, L., Nielsen, J., Kerkhoven, E.J., 2024. Reconstruction, simulation and analysis of enzyme-constrained metabolic models using GECKO Toolbox 3.0. Nat. Protoc. https://doi.org/10.5281/zenodo.7699818.

Choi, H.S., Lee, S.Y., Kim, T.Y., Woo, H.M., 2010. *In silico* identification of gene amplification targets for improvement of lycopene production. Appl. Environ. Microbiol. 76 (10), 3097–3105. https://doi.org/10.1128/AEM.00115-10.

Colombié, S., Dequin, S., Sablayrolles, J.M., 2003. Control of lactate production by expressing a bacterial *LDH* gene. Enzym. Microb. Technol. 33 (1), 38–46. https://doi.org/10.1016/S0141-0229(03)00082-6.

Curiel, J.A., Salvado, Z., Tronchoni, J., Morales, P., Rodrigues, A.J., Quiros, M., Gonzalez, R., 2016. Identification of target genes to control acetate yield during aerobic fermentation with *Saccharomyces cerevisiae*. Microb. Cell Factories 15 (1), 156. https://doi.org/10.1186/s12934-016-0555-y.

Dai, Z., Huang, M., Chen, Y., Siewers, V., Nielsen, J., 2018. Global rewiring of cellular metabolism renders *Saccharomyces cerevisiae* Crabtree negative. Nat. Commun. 9 (1), 3059. https://doi.org/10.1038/s41467-018-05409-9.

Dequin, S., Baptista, E., Barre, P., 1999. Acidification of grape musts by *Saccharomyces cerevisiae* wine yeast strains genetically engineered to produce lactic acid. Am. J. Enol. Vitic. 50, 45–50. https://doi.org/10.5344/ajev.1999.50.1.45.

Dinh, H.V., Maranas, C.D., 2023. Evaluating proteome allocation of *Saccharomyces cerevisiae* phenotypes with resource balance analysis. Metab. Eng. 77, 242–255. https://doi.org/10.1016/j.ymben.2023.04.009.

Eglinton, J.M., Heinrich, A.J., Pollnitz, A.P., Langridge, P., Henschke, P.A., de Barros Lopes, M., 2002. Decreasing acetic acid accumulation by a glycerol overproducing strain of *Saccharomyces cerevisiae* by deleting the *ALD6* aldehyde dehydrogenase gene. Yeast 19 (4), 295–301. https://doi.org/10.1002/yea.834.

Fujitomi, K., Sanda, T., Hasunuma, T., Kondo, A., 2012. Deletion of the *PHO13* gene in *Saccharomyces cerevisiae* improves ethanol production from lignocellulosic hydrolysate in the presence of acetic and formic acids, and furfural. Bioresour. Technol. 111, 161–166. https://doi.org/10.1016/j.biortech.2012.01.161.

Gietz, R.D., Schiestl, R.H., 2007. High-efficiency yeast transformation using the LiAc/SS carrier DNA/PEG method. Nat. Protoc. 2 (1), 31–34. https://doi.org/10.1038/nprot.2007.13.

Gietz, R.D., Sugino, A., 1988. New yeast-*Escherichia coli* shuttle vectors constructed with in vitro mutagenized yeast genes lacking six-base pair restriction sites. Gene 74 (2), 527–534. https://doi.org/10.1016/0378-1119(88)90185-0.

Guaragnella, N., Bettiga, M., 2021. Acetic acid stress in budding yeast: from molecular mechanisms to applications. Yeast 38 (7), 391–400. https://doi.org/10.1002/yea.3651.

Han, Y., Tafur Rangel, A., Pomraning, K.R., Kerkhoven, E.J., Kim, J., 2023. Advances in genome-scale metabolic models of industrially important fungi. Curr. Opin. Biotechnol. 84, 103005 https://doi.org/10.1016/j.copbio.2023.103005.

Hetényi, K., Németh, A., Sevella, B., 2011. Role of pH-regulation in lactic acid fermentation: second steps in a process improvement. Chem. Eng. Process 50 (3), 293–299. https://doi.org/10.1016/j.cep.2011.01.008.

Imai, T., Ohno, T., 1995. The Relationship between viability and intracellular pH in the yeast *Saccharomyces cerevisiae*. Appl. Environ. Microbiol. 61 (10), 3604–3608. https://doi.org/10.1128/aem.61.10.3604-3608.1995.

Ishida, N., Saitoh, S., Ohnishi, T., Tokuhiro, K., Nagamori, E., Kitamoto, K., Takahashi, H., 2006a. Metabolic engineering of *Saccharomyces cerevisiae* for efficient production of pure L-(+)-lactic acid. Appl. Biochem. Biotechnol. 131, 795–807. https://doi.org/10.1385/ABAB:131:1:795.

Ishida, N., Saitoh, S., Onishi, T., Tokuhiro, K., Nagamori, E., Kitamoto, K., Takahashi, H., 2006b. The effect of pyruvate decarboxylase gene knockout in *Saccharomyces cerevisiae* on L-lactic acid production. Biosci. Biotechnol. Biochem. 70 (5), 1148–1153. https://doi.org/10.1271/bbb.70.1148.

Ishida, N., Suzuki, T., Tokuhiro, K., Nagamori, E., Onishi, T., Saitoh, S., Kitamoto, K., Takahashi, H., 2006c. D-lactic acid production by metabolically engineered *Saccharomyces cerevisiae*. J. Biosci. Bioeng. 101 (2), 172–177. https://doi.org/10.1263/jbb.101.172.

Jang, B.K., Ju, Y., Jeong, D., Jung, S.K., Kim, C.K., Chung, Y.S., Kim, S.R., 2021. L-Lactic acid production using engineered *Saccharomyces cerevisiae* with improved organic acid tolerance. J Fungi (Basel) 7 (11) https://doi.org/10.3390/jof7110928.

Jin, Y.S., Alper, H., Yang, Y.T., Stephanopoulos, G., 2005. Improvement of xylose uptake and ethanol production in recombinant *Saccharomyces cerevisiae* through an inverse metabolic engineering approach. Appl. Environ. Microbiol. 71 (12), 8249–8256. https://doi.org/10.1128/AEM.71.12.8249-8256.2005.

Jin, Y.S., Jeffries, T.W., 2004. Stoichiometric network constraints on xylose metabolism by recombinant *Saccharomyces cerevisiae*. Metab. Eng. 6 (3), 229–238. https://doi.org/10.1016/j.ymben.2003.11.006.

Jin, Y.S., Ni, H., Laplaza, J.M., Jeffries, T.W., 2003. Optimal growth and ethanol production from xylose by recombinant *Saccharomyces cerevisiae* require moderate D-xylulokinase activity. Appl. Environ. Microbiol. 69 (1), 495–503. https://doi.org/10.1128/AEM.69.1.495-503.2003.

Jonsson, L.J., Alriksson, B., Nilvebrant, N.O., 2013. Bioconversion of lignocellulose: inhibitors and detoxification. Biotechnol. Biofuels 6, 16. https://doi.org/10.1186/1754-6834-6-16.

Karhumaa, K., Garcia Sanchez, R., Hahn-Hagerdal, B., Gorwa-Grauslund, M.F., 2007. Comparison of the xylose reductase-xylitol dehydrogenase and the xylose isomerase pathways for xylose fermentation by recombinant *Saccharomyces cerevisiae*. Microb. Cell Factories 6, 5. https://doi.org/10.1186/1475-2859-6-5.

Kerkhoven, E.J., 2022. Advances in constraint-based models: methods for improved predictive power based on resource allocation constraints. Curr. Opin. Microbiol. 68, 102168 https://doi.org/10.1016/j.mib.2022.102168.

Kim, S.R., Skerker, J.M., Kang, W., Lesmana, A., Wei, N., Arkin, A.P., Jin, Y.S., 2013. Rational and evolutionary engineering approaches uncover a small set of genetic changes efficient for rapid xylose fermentation in *Saccharomyces cerevisiae*. PLoS One 8 (2), e57048. https://doi.org/10.1371/journal.pone.0057048.

Kim, S.R., Xu, H., Lesmana, A., Kuzmanovic, U., Au, M., Florencia, C., Oh, E.J., Zhang, G., Kim, K.H., Jin, Y.S., 2015. Deletion of *PHO13*, encoding haloacid dehalogenase type IIA phosphatase, results in upregulation of the pentose phosphate pathway in *Saccharomyces cerevisiae*. Appl. Environ. Microbiol. 81 (5), 1601–1609. https://doi.org/10.1128/AEM.03474-14.

Krebs, H.A., Wiggins, D., Stubbs, M., Sols, A., Bedoya, F., 1983. Studies on the mechanism of the antifungal action of benzoate. Biochem. J. 214 (3), 657–663. https://doi.org/10.1042/bj2140657.

Lam, F.H., Turanli-Yildiz, B., Liu, D., Resch, M.G., Fink, G.R., Stephanopoulos, G., 2021. Engineered yeast tolerance enables efficient production from toxified lignocellulosic feedstocks. Sci. Adv. 7 (26) https://doi.org/10.1126/sciadv.abf7613.

Lane, S., Turner, T.L., Jin, Y.S., 2023. Glucose assimilation rate determines the partition of flux at pyruvate between lactic acid and ethanol in *Saccharomyces cerevisiae*. Biotechnol. J. 18 (4), E2200535 https://doi.org/10.1002/biot.202200535.

Lee, J.W., Yook, S., Koh, H., Rao, C.V., Jin, Y.S., 2021. Engineering xylose metabolism in yeasts to produce biofuels and chemicals. Curr. Opin. Biotechnol. 67, 15–25. https://doi.org/10.1016/j.copbio.2020.10.012.

Li, Y.C., Gou, Z.X., Liu, Z.S., Tang, Y.Q., Akamatsu, T., Kida, K., 2014. Synergistic effects of TAL1 over-expression and PHO13 deletion on the weak acid inhibition of xylose

fermentation by industrial *Saccharomyces cerevisiae* strain. Biotechnol. Lett. 36 (10), 2011–2021. https://doi.org/10.1007/s10529-014-1581-7.

Liang, L., Zhang, J., Lin, Z., 2007. Altering coenzyme specificity of Pichia stipitis xylose reductase by the semi-rational approach CASTing. Microb. Cell Factories 6, 36. https://doi.org/10.1186/1475-2859-6-36.

Liu, H., Wang, X., 2021. CRISPR-ERA: a webserver for guide rna design of gene editing and regulation. Methods Mol. Biol. 2189, 65–69. https://doi.org/10.1007/978-1-0716-0822-7_5.

Liu, C., Choi, B., Efimova, E., Nygård, Y., Santala, S., 2024. Enhanced upgrading of lignocellulosic substrates by coculture of *Saccharomyces cerevisiae* and *Acinetobacter baylyi* ADP1. Biotechnol. Biofuels 17, 61. https://doi.org/10.1186/s13068-024-02510-8.

Liu, T., Sun, L., Zhang, C., Liu, Y., Li, J., Du, G., Lv, X., Liu, L., 2023. Combinatorial metabolic engineering and process optimization enables highly efficient production of L-lactic acid by acid-tolerant *Saccharomyces cerevisiae*. Bioresour. Technol. 379, 129023 https://doi.org/10.1016/j.biortech.2023.129023.

Lu, H., Li, F., Sanchez, B.J., Zhu, Z., Li, G., Domenzain, I., Marcisauskas, S., Anton, P.M., Lappa, D., Lieven, C., Beber, M.E., Sonnenschein, N., Kerkhoven, E.J., Nielsen, J., 2019. A consensus *S. cerevisiae* metabolic model Yeast 8 and its ecosystem for comprehensively probing cellular metabolism. Nat. Commun. 10 (1), 3586. https://doi.org/10.1038/s41467-019-11581-3.

Maas, R.H., Springer, J., Eggink, G., Weusthuis, R.A., 2008. Xylose metabolism in the fungus *Rhizopus oryzae*: effect of growth and respiration on L-lactic acid production. J. Ind. Microbiol. Biotechnol. 35, 569–578. https://doi.org/10.1007/s10295-008-0318-9.

Ni, H., Laplaza, J.M., Jeffries, T.W., 2007. Transposon mutagenesis to improve the growth of recombinant *Saccharomyces cerevisiae* on D-xylose. Appl. Environ. Microbiol. 73 (7), 2061–2066. https://doi.org/10.1128/AEM.02564-06.

Nickel, D., 2021. Process Development for Platform Chemical Production from Agricultural and Forestry Residues. Chalmers University of Technology. Ph.D. https://research.chalmers.se/en/publication/522191.

Novy, V., Brunner, B., Nidetzky, B., 2018. L-Lactic acid production from glucose and xylose with engineered strains of *Saccharomyces cerevisiae*: aeration and carbon source influence yields and productivities. Microb. Cell Factories 17 (1), 59. https://doi.org/10.1186/s12934-018-0905-z.

Ojo, A.O., de Smidt, O., 2023. Lactic acid: a comprehensive review of production to purification. Processes 11 (3). https://doi.org/10.3390/pr11030688.

Ookubo, A., Hirasawa, T., Yoshikawa, K., Nagahisa, K., Furusawa, C., Shimizu, H., 2008. Improvement of L-lactate production by *CYB2* gene disruption in a recombinant *Saccharomyces cerevisiae* strain under low pH condition. Biosci. Biotechnol. Biochem. 72 (11), 3063–3066. https://doi.org/10.1271/bbb.80493.

Oud, B., Flores, C.L., Gancedo, C., Zhang, X., Trueheart, J., Daran, J.M., Pronk, J.T., van Maris, A.J., 2012. An internal deletion in *MTH1* enables growth on glucose of pyruvate-decarboxylase negative, non-fermentative *Saccharomyces cerevisiae*. Microb. Cell Factories 11, 131. https://doi.org/10.1186/1475-2859-11-131.

Papapetridis, I., van Dijk, M., Dobbe, A.P., Metz, B., Pronk, J.T., van Maris, A.J., 2016. Improving ethanol yield in acetate-reducing *Saccharomyces cerevisiae* by cofactor engineering of 6-phosphogluconate dehydrogenase and deletion of *ALD6*. Microb. Cell Factories 15, 67. https://doi.org/10.1186/s12934-016-0465-z.

Piper, P., Calderon, C.O., Hatzixanthis, K., Mollapour, M., 2001. Weak acid adaptation: the stress response that confers yeasts with resistance to organic acid food preservatives. Microbiol-Sgm 147, 2635–2642. https://doi.org/10.1099/00221287-147-10-2635.

Reider Apel, A., Ouellet, M., Szmidt-Middleton, H., Keasling, J.D., Mukhopadhyay, A., 2016. Evolved hexose transporter enhances xylose uptake and glucose/xylose co-utilization in *Saccharomyces cerevisiae*. Sci. Rep. 6, 19512 https://doi.org/10.1038/srep19512.

Remize, F., Cambon, B., Barnavon, L., Dequin, S., 2003. Glycerol formation during wine fermentation is mainly linked to Gpd1p and is only partially controlled by the HOG pathway. Yeast 20 (15), 1243–1253. https://doi.org/10.1002/yea.1041.

Saitoh, S., Ishida, N., Onishi, T., Tokuhiro, K., Nagamori, E., Kitamoto, K., Takahashi, H., 2005. Genetically engineered wine yeast produces a high concentration of L-lactic acid of extremely high optical purity. Appl. Environ. Microbiol. 71 (5), 2789–2792. https://doi.org/10.1128/AEM.71.5.2789-2792.2005.

Sánchez, B.J., Li, F., Lu, H., 2018. SysBioChalmers/yeast-GEM: Yeast 7.8.0. Zenodo. https://zenodo.org/records/1494186.

Sato, T.K., Tremaine, M., Parreiras, L.S., Hebert, A.S., Myers, K.S., Higbee, A.J., Sardi, M., McIlwain, S.J., Ong, I.M., Breuer, R.J., Narasimhan, R.A., Mcgee, M.A., Dickinson, Q., La Reau, A., Xie, D., Tian, M.Y., Reed, J.L., Zhang, Y.P., Coon, J.J., Hittinger, C.T., Gasch, A.P., Landick, R., 2016. Directed evolution reveals unexpected epistatic interactions that alter metabolic regulation and enable anaerobic xylose use by *Saccharomyces cerevisiae*. PLoS Genet. 12 (10), e1006372 https://doi.org/10.1371/journal.pgen.1006372.

Singh, N., Singhania, R.R., Nigam, P.S., Dong, C.D., Patel, A.K., Puri, M., 2022. Global status of lignocellulosic biorefinery: challenges and perspectives. Bioresour. Technol. 344, 126415 https://doi.org/10.1016/j.biortech.2021.126415.

Skory, C.D., 2003. Lactic acid production by *Saccharomyces cerevisiae* expressing a *Rhizopus oryzae* lactate dehydrogenase gene. J. Ind. Microbiol. Biotechnol. 30 (1), 22–27. https://doi.org/10.1007/s10295-002-0004-2.

Song, J.Y., Park, J.S., Kang, C.D., Cho, H.Y., Yang, D., Lee, S., Cho, K.M., 2016. Introduction of a bacterial acetyl-CoA synthesis pathway improves lactic acid production in *Saccharomyces cerevisiae*. Metab. Eng. 35, 38–45. https://doi.org/10.1016/j.ymben.2015.09.006.

Srivastava, N., Singh, R., Singh, P., Ahmad, I., Singh, R.P., Rai, A.K., Asiri, M., Gupta, V.K., 2023. Recent advances on lignocellulosic bioresources and their valorization in

biofuels production: challenges and viability assessment. Environ. Technol. Innov. 29 https://doi.org/10.1016/j.eti.2023.103037.

Tokuhiro, K., Ishida, N., Nagamori, E., Saitoh, S., Onishi, T., Kondo, A., Takahashi, H., 2009. Double mutation of the *PDC1* and *ADH1* genes improves lactate production in the yeast *Saccharomyces cerevisiae* expressing the bovine lactate dehydrogenase gene. Appl. Microbiol. Biotechnol. 82 (5), 883–890. https://doi.org/10.1007/s00253-008-1831-5.

Turner, T.L., Zhang, G.C., Kim, S., Subramaniam, V., Steffen, D., Skory, C.D., Jang, J.Y., Yu, B.J., Jin, Y.S., 2015. Lactic acid production from xylose by engineered *Saccharomyces cerevisiae* without *PDC* or *ADH* deletion. Appl. Microbiol. Biotechnol. 99 (19), 8023–8033. https://doi.org/10.1007/s00253-015-6701-3.

Turner, T.L., Zhang, G.C., Oh, E.J., Subramaniam, V., Adiputra, A., Subramaniam, V., Skory, C.D., Jang, J.Y., Yu, B.J., Park, I., Jin, Y.S., 2016. Lactic acid production from cellobiose and xylose by engineered *Saccharomyces cerevisiae*. Biotechnol. Bioeng. 113 (5), 1075–1083. https://doi.org/10.1002/bit.25875.

Valli, M., Sauer, M., Branduardi, P., Borth, N., Porro, D., Mattanovich, D., 2006. Improvement of lactic acid production in *Saccharomyces cerevisiae* by cell sorting for high intracellular pH. Appl. Environ. Microbiol. 72 (8), 5492–5499. https://doi.org/10.1128/AEM.00683-06.

van Dijken, J.P., Weusthuis, R.A., Pronk, J.T., 1993. Kinetics of growth and sugar consumption in yeasts. Antonie Leeuwenhoek 63 (3–4), 343–352. https://doi.org/10.1007/BF00871229.

van Maris, A.J., Geertman, J.M., Vermeulen, A., Groothuizen, M.K., Winkler, A.A., Piper, M.D., van Dijken, J.P., Pronk, J.T., 2004. Directed evolution of pyruvate decarboxylase-negative *Saccharomyces cerevisiae*, yielding a C2-independent, glucose-tolerant, and pyruvate-hyperproducing yeast. Appl. Environ. Microbiol. 70 (1), 159–166. https://doi.org/10.1128/AEM.70.1.159-166.2004.

Van Vleet, J.H., Jeffries, T.W., Olsson, L., 2008. Deleting the para-nitrophenyl phosphatase (pNPPase), *PHO13*, in recombinant *Saccharomyces cerevisiae* improves growth and ethanol production on D-xylose. Metab. Eng. 10 (6), 360–369. https://doi.org/10.1016/j.ymben.2007.12.002.

Vanmarcke, G., Demeke, M.M., Foulquie-Moreno, M.R., Thevelein, J.M., 2021. Identification of the major fermentation inhibitors of recombinant 2G yeasts in diverse lignocellulose hydrolysates. Biotechnol. Biofuels 14 (1), 92. https://doi.org/10.1186/s13068-021-01935-9.

Verho, R., Londesborough, J., Penttila, M., Richard, P., 2003. Engineering redox cofactor regeneration for improved pentose fermentation in *Saccharomyces cerevisiae*. Appl. Environ. Microbiol. 69 (10), 5892–5897. https://doi.org/10.1128/AEM.69.10.5892-5897.2003.

Viegas, C.A., Almeida, P.F., Cavaco, M., Sa-Correia, I., 1998. The H+-ATPase in the plasma membrane of *Saccharomyces cerevisiae* is activated during growth latency in octanoic acid-supplemented medium accompanying the decrease in intracellular pH and cell viability. Appl. Environ. Microbiol. 64 (2), 779–783. https://doi.org/10.1128/AEM.64.2.779-783.1998.

Wang, H., Marcisauskas, S., Sanchez, B.J., Domenzain, I., Hermansson, D., Agren, R., Nielsen, J., Kerkhoven, E.J., 2018. Raven 2.0: a versatile toolbox for metabolic network reconstruction and a case study on Streptomyces coelicolor. PLoS Comput. Biol. 14, e1006541 https://doi.org/10.1371/journal.pcbi.1006541.

Watanabe, S., Kodaki, T., Makino, K., 2005. Complete reversal of coenzyme specificity of xylitol dehydrogenase and increase of thermostability by the introduction of structural zinc. J. Biol. Chem. 280 (11), 10340–10349. https://doi.org/10.1074/jbc.M409443200.

Westman, J.O., Bonander, N., Taherzadeh, M.J., Franzen, C.J., 2014. Improved sugar co-utilisation by encapsulation of a recombinant *Saccharomyces cerevisiae* strain in alginate-chitosan capsules. Biotechnol. Biofuels 7, 102. https://doi.org/10.1186/1754-6834-7-102.

Xu, H., Kim, S., Sorek, H., Lee, Y., Jeong, D., Kim, J., Oh, E.J., Yun, E.J., Wemmer, D.E., Kim, K.H., Kim, S.R., Jin, Y.S., 2016. *PHO13* deletion-induced transcriptional activation prevents sedoheptulose accumulation during xylose metabolism in engineered *Saccharomyces cerevisiae*. Metab. Eng. 34, 88–96. https://doi.org/10.1016/j.ymben.2015.12.007.

Yang, P.B., Tian, Y., Wang, Q., Cong, W., 2015. Effect of different types of calcium carbonate on the lactic acid fermentation performance of *Lactobacillus lactis*. Biochem. Eng. J. 98, 38–46. https://doi.org/10.1016/j.bej.2015.02.023.

Yankov, D., 2022. Fermentative lactic acid production from lignocellulosic feedstocks: from source to purified product. Front. Chem. 10, 823005 https://doi.org/10.3389/fchem.2022.823005.

Ye, S., Jeong, D., Shon, J.C., Liu, K.H., Kim, K.H., Shin, M., Kim, S.R., 2019. Deletion of *PHO13* improves aerobic L-arabinose fermentation in engineered *Saccharomyces cerevisiae*. J. Ind. Microbiol. Biotechnol. 46 (12), 1725–1731. https://doi.org/10.1007/s10295-019-02233-y.